

8. Leznoff, C. C. & Lever, A. B. P. (eds) *Phthalocyanines: Properties and Applications* (VCH, New York, 1989).
9. Wang, L. S., Ding, C. F., Wang, X. B. & Barlow, S. E. Photodetachment photoelectron spectroscopy of multiply charged anions using electrospray ionization. *Rev. Sci. Instrum.* **70**, 1957–1966 (1999).
10. Berkowitz, J. Photoelectron spectroscopy of phthalocyanine vapors. *J. Chem. Phys.* **70**, 2819–2828 (1979).
11. Brown, C. J. Crystal structure of β -copper phthalocyanine. *J. Chem. Soc. A* 2488–2493 (1968).
12. Rosa, A. & Baerends, E. J. Metal-macrocycle interaction in phthalocyanines: density functional calculations of ground and excited states. *Inorg. Chem.* **33**, 584–595 (1994).
13. PC Spartan Plus 5.1 (Wavefunction, Inc., Von Carman Ave., Irvine, California 92612, USA).
14. Stewart, J. J. Optimization of parameters for semiempirical methods II: Applications. *J. Comput. Chem.* **10**, 221–264 (1989); MOPAC: A semiempirical molecular orbital program. *J. Comput. Aided Mol. Design* **4**, 1–105 (1990).
15. D'Haennens, I. J. in *Encyclopedia of Physics* (eds Lerner, R. G. & Trigg, G. L.) 1251–1253 (VCH, New York, 1991).
16. Hodgson, P. E., Gadioli, E. & Erba, E. G. *Introductory Nuclear Physics* (Clarendon, Oxford, 1997).
17. Scheller, M. K. & Cederbaum, L. S. A construction principle for stable multiply charged molecular anions in the gas phase. *Chem. Phys. Lett.* **216**, 141–146 (1993).
18. Weikert, H.-G. & Cederbaum, L. S. Free doubly negative tetrahalides. *J. Chem. Phys.* **99**, 8877–8891 (1993).
19. Boldyrev, A. I., Gutowski, M. & Simons, J. Small multiply charged anions as building blocks in chemistry. *Acc. Chem. Res.* **29**, 497–502 (1996).
20. Vekey, K. Multiply charged ions. *Mass Spectrom. Rev.* **14**, 195–225 (1995).
21. Brechignac, C., Cahuzac, P., Kebaili, N. & Leygnier, J. Temperature effects in the Coulombic fission of strontium clusters. *Phys. Rev. Lett.* **81**, 4612–4615 (1998).
22. Schroder, D., Harvey, J. N. & Schwarz, H. Long-lived, multiply charged diatomic TiF^{n-} ions ($n = 1-3$). *J. Phys. Chem. A* **102**, 3639–3642 (1998).

Acknowledgements. We thank R. S. Disselkamp for discussions and K. Ferris for help in the theoretical calculations. This work was supported by the US Department of Energy, Office of Basic Energy Sciences, Chemical Sciences Division and is conducted at the Pacific Northwest National Laboratory, operated for the US Department of Energy by Battelle Memorial Institute. L.-S.W. is an Alfred P. Sloan research fellow.

Correspondence and requests for materials should be addressed to L.-S.W. (e-mail: ls.wang@pnl.gov).

Dual modes of the carbon cycle since the Last Glacial Maximum

H. Jesse Smith*, H. Fischer*†, M. Wahlen*, D. Mastroianni* & B. Deck*

* Scripps Institution of Oceanography, University of California San Diego, La Jolla, California 92093-0220, USA

The most conspicuous feature of the record of past climate contained in polar ice is the rapid warming which occurs after long intervals of gradual cooling. During the last four transitions from glacial to interglacial conditions, over which such abrupt warmings occur, ice records indicate that the CO_2 concentration of the atmosphere increased by roughly 80 to 100 parts per million by volume (refs 1–4). But the causes of the atmospheric CO_2 concentration increases are unclear. Here we present the stable-carbon-isotope composition ($\delta^{13}\text{C}$) of CO_2 extracted from air trapped in ice at Taylor Dome, Antarctica, from the Last Glacial Maximum to the onset of Holocene times. The global carbon cycle is shown to have operated in two distinct primary modes on the timescale of thousands of years, one when climate was changing relatively slowly and another when warming was rapid, each with a characteristic average stable-carbon-isotope composition of the net CO_2 exchanged by the atmosphere with the land and oceans. $\delta^{13}\text{C}$ increased between 16.5 and 9 thousand years ago by slightly more than would be estimated to be caused by the physical effects of a 5°C rise in global average sea surface temperature driving a CO_2 efflux from the ocean, but our data do not allow specific causes to be constrained.

Carbon dioxide in the atmosphere causes a radiative forcing second only to water vapour, and so may be a central agent in climate change. Polar ice cores contain a detailed record of climate-

related variables which extends more than 400,000 years into the past⁴, and are especially valuable for studying variations of atmospheric CO_2 as they contain an effectively direct record, unlike atmospheric proxies such as marine carbonates or preserved organic material⁵ which may also reflect biological effects. Ice cores from Antarctica, such as those of Taylor Dome and Vostok, are the best sources for palaeoatmospheric CO_2 measurements because they contain only small amounts of the kinds of chemical impurities, such as carbonate dust or organic acids, that may lead to contamination by *in situ* CO_2 production^{2,6–8}. Taylor Dome ice has the additional advantage that the entire 554-m-long core is from above the depth at which air trapped in bubbles in the ice forms gas-ice clathrates. This feature is important because, as we have found, the accuracy of $\delta^{13}\text{C}$ measurements performed on bubble-free ice may be affected by the presence of clathrates. ($\delta^{13}\text{C}$ is defined in Methods.) We have measured the CO_2 concentration and $\delta^{13}\text{C}$ of air trapped in ice from Taylor Dome, Antarctica, across the last glacial termination in order to develop a time series for the carbon-isotope composition of atmospheric CO_2 and to constrain the mechanisms of carbon cycling between the main sources and sinks of atmospheric CO_2 .

The atmospheric CO_2 concentration data^{3,9} (Fig. 1) form a record comparable to that from Byrd and Vostok^{1,2}. The salient features include a low but variable concentration of atmospheric CO_2 between 27.1 and 18.0 kyr BP (thousand years before present, where “present” is defined as AD 1950), when it varied between 186 and 201 parts per million by volume (p.p.m.v.); a rise, at a fairly constant rate, from 190 p.p.m.v. at 17.0 kyr BP to an early Holocene local maximum of 268 p.p.m.v. at 10.6 kyr BP, punctuated by a shallow minimum at 16.1 kyr BP and a drop of 8 p.p.m.v. between 14 and 13 kyr BP which may be related to the Antarctic Cold Reversal³; an 8 p.p.m.v. decrease, from 268 p.p.m.v. at 10.6 kyr BP to 260 p.p.m.v. at 9.1 kyr BP, followed by a rise to the pre-industrial level of about 280 p.p.m.v. (as discussed in detail by Indermühle *et al.*⁹). These data can be combined with the carbon-isotope composition of the CO_2 to give a better picture of how the carbon cycle operated during this time.

The main features of the carbon-isotope record shown in Fig. 1 include a 0.5‰ drop in $\delta^{13}\text{C}$ between 18.0 and 16.5 kyr BP, and the subsequent increase of 0.7‰, from -7.0 ‰ to -6.3 ‰, between 16.5 and 9.1 kyr BP, which is interrupted by two local $\delta^{13}\text{C}$ minima at approximately 13 and 10 kyr BP. The minimum-to-maximum $\delta^{13}\text{C}$ increase began 1,000 to 2,000 years after CO_2 began to rise, and continued to rise for $\sim 3,000$ years after the CO_2 concentration maximum at 10.6 kyr BP, which we interpret as a consequence of the bimodality of carbon cycling (discussed below) rather than a decoupling of CO_2 concentrations from carbon-isotope compositions. Furthermore, there appears to have been an extended local minimum in $\delta^{13}\text{C}$ between 13.4 and 12.3 kyr BP that accompanied the Younger Dryas¹⁰ but was not concurrent with the CO_2 concentration drop at 14 kyr BP. The 0.16‰ difference between the average $\delta^{13}\text{C}$ values of the Last Glacial Maximum (LGM) and Holocene (see Fig. 2 legend for an explanation of these groupings) is similar to the increase of 0.19 ± 0.18 ‰ estimated by Leuenberger *et al.*¹¹ to have occurred between the period 20–40 kyr BP and the early Holocene. These data show, however, that there was a significant drop in $\delta^{13}\text{C}$ between the end of the LGM and the beginning of the transition, and that the subsequent rise into the early Holocene was much larger than the difference between average values for the LGM and Holocene. Moreover, inferences about the carbon cycle drawn from the comparison of the LGM and Holocene averages may be misleading because there was significant variability within each of those periods, and the averages depend strongly on the interval chosen to calculate them. Finally, the variability of $\delta^{13}\text{C}$ before 17.5 kyr BP and after 10.3 kyr BP, 0.33‰ and 0.37‰, respectively, is about half of the magnitude of the

† Present address: Alfred-Wegener-Institute for Polar and Marine Research, Columbusstrasse, D-27515 Bremerhaven, Germany.

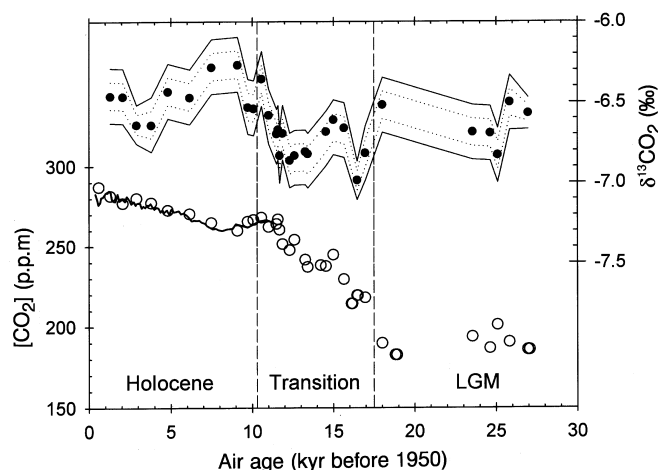


Figure 1 $\delta^{13}\text{CO}_2$ and CO_2 -concentration trends. The data are based on measurements of air trapped in ice from Taylor Dome, Antarctica, and are plotted against air age. Upper curve, $\delta^{13}\text{CO}_2$ values (filled circles) within envelopes of 1σ and 2σ uncertainty (indicated as dotted and solid lines, respectively; see the Methods section for details). Lower curve, CO_2 concentration data shown as open circles were measured in our laboratory at SIO³, while the solid line shown in the Holocene (for comparison) is the higher-resolution record of Indermühle *et al.*⁹. The age axis is divided into three intervals, called "LGM", "transition", and "Holocene" on the basis of CO_2 concentrations and generally accepted ages for these periods. The LGM group includes all of the points with air ages between 27.1 and 18.0 kyr BP, the youngest being the last with a CO_2 concentration below the highest value of the older samples. The transition group includes the points with ages between 17.0 and 10.6 kyr BP, where the local CO_2 maximum which we use to define the start of the Holocene occurs. The Holocene group includes all the points with ages between 10.1 and 1.3 kyr BP (the youngest sample measured for $\delta^{13}\text{CO}_2$). The boundaries between the LGM and the transition, and between the transition and the Holocene, chosen here to fall at 17.5 and 10.3 kyr BP, respectively, are shown as vertical dashed lines.

increase that occurs during the transition, indicating that carbon cycling also varied considerably over shorter timescales.

The atmospheric portion of the carbon cycle is extremely dynamic; ~20% of the CO_2 in the atmosphere is exchanged with the ocean and terrestrial biosphere every year (ref. 12), so the atmosphere responds very quickly to changes in CO_2 cycling between these three reservoirs. The exchange of carbon can affect the isotopic composition of atmospheric CO_2 for two reasons. First, the reservoirs have different carbon-isotope compositions (the $\delta^{13}\text{CO}_2$ of the ocean is close to 0‰, the terrestrial biosphere has a $\delta^{13}\text{CO}_2$ of approximately -25‰ and that of pre-industrial atmosphere was approximately -6.5‰; ref. 13). Second, each flux of CO_2 between the atmosphere and either the ocean or the terrestrial biosphere is accompanied by a different carbon-isotope fractionation, resulting in isotopically unique values of $\delta^{13}\text{CO}_2$ for each transfer. Consequently, variations in the carbon-isotope composition of atmospheric CO_2 can be caused by a net flux of carbon between reservoirs, or by a change in the isotopic fractionation associated with a particular atmospheric flux. It also follows from this that the carbon-isotope composition of the net atmospheric CO_2 exchanged, $\delta^{13}\text{CO}_2(\text{ex})$, is a function of the relative strengths of processes which transfer CO_2 into and out of the atmosphere, so different $\delta^{13}\text{CO}_2(\text{ex})$ values indicate different balances of processes. When a unique balance of processes persists over thousands of years, as indicated by a unique $\delta^{13}\text{CO}_2(\text{ex})$, we refer to it as a 'mode' of the carbon cycle.

In order to examine more closely the implications of the time series shown in Fig. 1, it is advantageous to consider the three data groups (LGM, transition and Holocene) individually. Doing so in

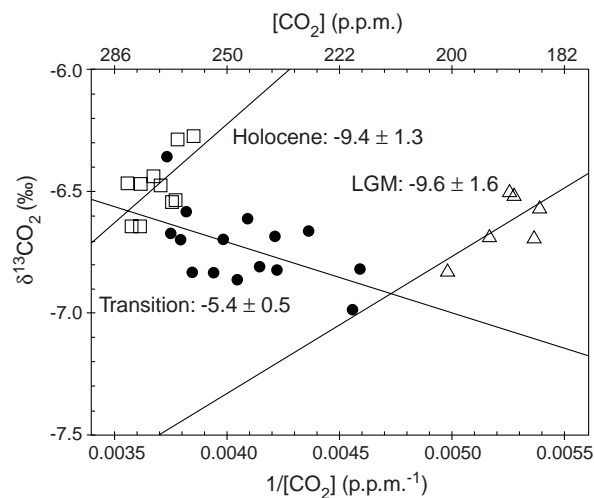


Figure 2 Mixing diagram for Taylor Dome samples: $1/[\text{CO}_2]$ is plotted against $\delta^{13}\text{CO}_2$. The data are divided into three groups, as described in the figure: the LGM group (open triangles, 6 $\delta^{13}\text{CO}_2$ points), the transition group (filled circles, 15 $\delta^{13}\text{CO}_2$ points), and the Holocene group (open squares, 10 $\delta^{13}\text{CO}_2$ points). The y -intercept of the regression line through each of the three groups of data, along with the corresponding 1σ uncertainty for each value, indicates the $\delta^{13}\text{C}$ of the CO_2 exchanged by the atmosphere, $\delta^{13}\text{CO}_2(\text{ex})$, and is shown on the figure.

Fig. 2 reveals a relationship between the concentration of atmospheric CO_2 and its carbon-isotope composition during each of these intervals. (Figure 2 is a mixing diagram, where the inverse CO_2 concentration is plotted against $\delta^{13}\text{CO}_2$, so that addition or removal of CO_2 with a given $\delta^{13}\text{C}$ would appear as a nearly straight line with the y -intercept approximately equal to the isotopic composition of the net CO_2 added to, or subtracted from, the atmosphere.) The coherent trends displayed by these groups show that the carbon cycle has operated in two distinct modes over the past 27 kyr, one during the Holocene, and possibly the LGM as well, when the average $\delta^{13}\text{C}$ of net CO_2 exchanged was approximately -10‰, and another during the transition, when the average $\delta^{13}\text{C}$ of net CO_2 exchanged was approximately -5‰. In other words, during the period of relatively stable, slowly changing climate of the Holocene, the carbon of the net exchanged atmospheric CO_2 was isotopically lighter than the average atmospheric value (that is, $d\delta^{13}\text{CO}_2/d\text{CO}_2$ was negative). In contrast, during the period of rapidly changing climate of the transition the net exchanged CO_2 was isotopically heavier ($d\delta^{13}\text{CO}_2/d\text{CO}_2$ was positive). Therefore, these data suggest that the carbon cycle has operated in two primary modes over the past 27 kyr, one when climate is changing only slowly and another when rapid warming occurs, and that although there are clearly other processes which have affected atmospheric CO_2 over the past 27 kyr, as is evident from the scatter in the data shown in Fig. 2, those transient variations did not overwhelm the longer-term trends.

Many schemes have been advanced to account for the magnitude of the rise in the concentration of atmospheric CO_2 during deglaciations (see, for example, Broecker¹⁴ for a critical review), although none seem to be uniquely sufficient. Two factors which must be included in any analysis of the glacial-interglacial increase in atmospheric CO_2 content, however, are a rise in sea surface temperature (SST) and a decrease in ocean salinity (S). In the range of SST, atmospheric CO_2 concentration and salinity appropriate for this study, changes in SST affect both atmospheric p_{CO_2} and $\delta^{13}\text{CO}_2$, by approximately 4.2% per °C (ref. 15) and 0.11–0.13‰ per °C (ref. 16), respectively, while changes in salinity alter p_{CO_2} by 10 p.p.m.v. per ‰ without affecting its $\delta^{13}\text{C}$ (ref. 17). Measurements performed on tropical corals show that SST increased by 5–6 °C from

the last peak-glacial period to the early Holocene¹⁸, significantly more than the earlier estimate of 1–2 °C by CLIMAP¹⁹, while the change in ocean salinity, estimated from sea level change²⁰, was approximately –1.4‰. Assuming a global average ΔSST (sea surface temperature change) of 5 °C, the combined effects of temperature and salinity changes should have resulted in increases in the concentration and δ¹³CO₂ of roughly 30 p.p.m.v. and 0.6‰, respectively. If this were true, then all other processes which caused variations in atmospheric CO₂ must together have increased its concentration by ~50 p.p.m.v. and its δ¹³CO₂ by only 0.1‰. A 2 °C global average ΔSST, on the other hand, would have caused no significant change in the concentration of atmospheric CO₂ and increased δ¹³CO₂ by roughly 0.2‰, leaving unexplained an approximately 80 p.p.m. concentration increase and a 0.5‰ δ¹³CO₂ increase. Adding these changes to the 0.3‰ whole-ocean δ¹³CO₂ increase which is thought to have accompanied deglaciation²¹, the expected increase in atmospheric δ¹³CO₂ would be between 0.9‰ and 0.6‰, depending on whether a ΔSST of 5 or 2 °C is assumed. The observed increase of 0.7‰ would seem to imply, then, that it is not necessary to invoke a large decrease in surface ocean productivity (which would lower atmospheric δ¹³CO₂ to values more negative than are observed) to explain the δ¹³CO₂ increase during the transition. What does become necessary, then, is to explain the 0.5‰ drop seen between 18 and 16.5 kyr BP.

In the broadest sense, the atmospheric δ¹³CO₂ record presented here points to the ocean as the predominant source of atmospheric CO₂ during the transition. This interpretation follows from two observations. First, even if a change in average global SST alone had caused the increase in δ¹³CO₂, a realistic ΔSST would have resulted in an increase of atmospheric CO₂ concentration of less than half of what is observed, so there must have been other sources of CO₂ during that time. Second, because δ¹³CO₂ was increasing at a rate equal to or greater than that which rising SST alone would have caused, the additional net CO₂ flux must have had a δ¹³CO₂ equal to, or greater than, that of the coexisting atmosphere, eliminating the terrestrial biosphere as a possible source. The most likely explanation for this is an enhanced flux from the ocean (with a δ¹³C close to that of the atmosphere) which transferred CO₂ into the atmosphere at a rate greater than the concurrent uptake of isotopically light CO₂ by an expanding terrestrial biosphere. Unfortunately, the constraints imposed by these data are insufficient to allow the identification of a specific cause for the increased flux of CO₂ from the ocean to the atmosphere. A better understanding of the carbon cycle depends not only on better models, but on additional experimental constraints on the carbon system, particularly more precise data about changes in SST, the size and composition of the terrestrial biosphere, the growth of coral reefs during periods of sea level rise, marine productivity and the chemical composition of the oceans. □

Methods

All samples were taken from Taylor Dome, Antarctica (77°04' S, 158°43' E, elevation 2,374 m), drilled in 1993/94. The methods used for determining the CO₂ concentration of air trapped in ice and the measurement of its carbon-isotope composition are described in detail elsewhere^{22,23}. CO₂ concentration measurements have an internal precision of ±3 p.p.m.v. (2σ) and are calculated by comparison to three standards of precisely known compositions which are run with every sample. The Craig-corrected²⁴ carbon-isotope measurements, performed on our VG Prism II isotope ratio mass spectrometer, have a 1σ precision of ±0.075‰, based on numerous analyses of the CO₂ separated from an atmospheric air standard exposed to uncrushed ice, in order to simulate the conditions of a sample run and to check for fractionation during extraction. δ¹³CO₂ is reported in normal δ notation as the per mil difference between the isotopic composition of the sample and standard VPDB carbon, [(¹³C/¹²C)_{sample} / (¹³C/¹²C)_{VPDB} – 1] × 1,000.

The δ¹³CO₂ values reported here have been corrected for the gravitational separation of gases of different masses in the firm, and for the presence of N₂O (which results in isobaric interferences with CO₂ during mass spectrometry).

Gravitational separation in the firm^{25,26} was determined by using the values of δ¹⁵N₂ of air trapped in Taylor Dome ice from Sucher²⁷, following the approach of Sowers and Bender²⁸. The gravitational correction for δ¹³CO₂ is ~0.005‰ per m. C-isotope data are corrected for the presence of N₂O on the basis of calibrations performed in our laboratory on CO₂–N₂O mixtures. The N₂O concentrations of atmospheric air used for this correction, adapted from Leuenberger and Siegenthaler²⁹, are linear interpolations of the following concentrations and dates: 275 p.p.b. (0–9.25 yr BP), 200 p.p.b. (16.1–27.2 kyr BP). The N₂O correction is ~0.001‰ per p.p.b. of N₂O. The total 1σ uncertainty in the reported δ¹³CO₂ of a single sample, including uncertainties in the gravitational and N₂O corrections, is 0.085‰. Duplicate analyses of samples with air ages of 2.19 and 17.2 kyr BP have a 1σ uncertainty of 0.060‰ and a triplicate analysis of the sample with an air age of 27.4 kyr BP has a 1σ uncertainty of 0.049‰. The depth–age scale and air age–ice age differences were calculated using a combination of flow modelling, correlating variations in the δ¹⁸O of the ice with the well-dated GISP2, and matching atmospheric CH₄ concentrations and δ¹⁸O of O₂ with variations seen in GISP2³⁰.

Received 8 October 1998; accepted 7 June 1999.

- Barnola, J. M., Raynaud, D., Korotkevich, Y. S. & Lorius, C. Vostok ice core provides 160,000-year record of atmospheric CO₂. *Nature* **329**, 408–414 (1987).
- Neffel, A., Oeschger, H., Staffelbach, T. & Stauffer, B. CO₂ record in the Byrd ice core 50,000–5,000 years BP. *Nature* **331**, 609–611 (1988).
- Fischer, H., Wahlen, M., Smith, H. J., Mastroianni, D. & Deck, B. Ice core records of atmospheric CO₂ around the last three glacial terminations. *Science* **283**, 1712–1714 (1999).
- Petit, J. R. *et al.* Climate and atmospheric history of the past 420,000 years from the Vostok ice core, Antarctica. *Nature* **399**, 429–436 (1999).
- Marino, B., McElroy, M. B., Salawitch, R. J. & Spaulding, W. G. Glacial-to-interglacial variations in the carbon isotopic composition of atmospheric CO₂. *Nature* **357**, 461–466 (1992).
- Anklin, M., Barnola, J.-M., Schwander, J., Stauffer, B. & Raynaud, D. Processes affecting the CO₂ concentrations measured in Greenland ice. *Tellus B* **47**, 461–470 (1995).
- Delmas, R. J. A natural artefact in Greenland ice core CO₂ measurements. *Tellus B* **45**, 391–396 (1993).
- Barnola, J. M. *et al.* CO₂ evolution during the last millennium as recorded by Antarctic and Greenland ice. *Tellus B* **47**, 264–272 (1995).
- Indermühle, A. *et al.* Holocene carbon-cycle dynamics based on CO₂ trapped in ice at Taylor Dome, Antarctica. *Nature* **398**, 121–126 (1999).
- Fairbanks, R. G. The age and origin of the “Younger Dryas Climate Event” in Greenland ice cores. *Paleoceanography* **5**, 937–948 (1990).
- Leuenberger, M., Siegenthaler, U. & Langway, C. C. Carbon isotope composition of atmospheric CO₂ during the last ice age from an Antarctic ice core. *Nature* **357**, 488–490 (1992).
- Tans, P. P., Berry, J. A. & Keeling, R. F. Oceanic ¹³C/¹²C observations: a new window on ocean CO₂ uptake. *Glob. Biogeochem. Cycles* **7**, 353–368 (1993).
- Friedli, H., Lutschner, H., Oeschger, H., Siegenthaler, U. & Stauffer, B. Ice core record of the ¹³C/¹²C of atmospheric CO₂ in the past two centuries. *Nature* **324**, 237–238 (1986).
- Broecker, W. S. & Henderson, G. M. The sequence of events surrounding Termination II and their implications for the cause of glacial-interglacial CO₂ changes. *Paleoceanography* **13**, 352–364 (1998).
- Takahashi, T., Olfsson, J., Goddard, J. G., Chipman, D. W. & Sutherland, S. C. Seasonal variation of CO₂ and nutrients in the high-latitude surface oceans: a comparative study. *Glob. Biogeochem. Cycles* **7**, 843–878 (1993).
- Mook, W. G., Bommerson, J. C. & Staverman, W. H. Carbon isotope fractionation between dissolved bicarbonate and gaseous carbon dioxide. *Earth Planet. Sci. Lett.* **22**, 169–176 (1974).
- Weiss, R. F. Carbon dioxide in water and seawater: the solubility of a non-ideal gas. *Mar. Chem.* **2**, 203–215 (1974).
- Guilderson, T. P., Fairbanks, R. G. & Rubenstone, J. L. Tropical temperature variations since 20,000 years ago: modulating interhemispheric climate change. *Science* **263**, 663–665 (1994).
- CLIMAP Project Members *Seasonal Reconstructions of the Earth's Surface at the Last Glacial Maximum* (Map and Chart Ser., MC-36, Geol. Soc. Am., Boulder, 1981).
- Fairbanks, R. G. A 17,000-year glacio-eustatic sea level record—implication of glacial melting rates on the Younger Dryas Event and deep-ocean circulation. *Nature* **342**, 637–642 (1989).
- Duplessy, J. C. *et al.* Deepwater source variations during the last climatic cycle and their impact on the global deepwater circulation. *Paleoceanography* **3**, 343–360 (1988).
- Wahlen, M., Allen, D. & Deck, B. Initial measurements of CO₂ concentrations (1530 to 1940 AD) in air occluded in the GISP 2 ice core from central Greenland. *Geophys. Res. Lett.* **18**, 1457–1460 (1991).
- Smith, H. J., Wahlen, M., Mastroianni, D. & Taylor, K. C. The CO₂ concentration of air trapped in GISP2 ice from the LGM-Holocene transition. *Geophys. Res. Lett.* **24**, 1–4 (1997).
- Craig, H. Isotopic standards for carbon and oxygen and correction factors for mass-spectrometric analysis of carbon dioxide. *Geochim. Cosmochim. Acta* **12**, 133–149 (1957).
- Craig, H., Horibe, Y. & Sowers, T. Gravitational separation of gases and isotopes in polar ice caps. *Science* **242**, 1675–1678 (1988).
- Schwander, J. *The Environmental Record in Glaciers and Ice Sheets* (eds Oeschger, H. and Langway, C. C.) 53–67 (Wiley and Sons, New York, 1989).
- Sucher, C. *Trapped Gases in the Taylor Dome Ice Core: Implications for East Antarctic Climate Change*. Thesis, Univ. Rhode Island (1997).
- Sowers, T. & Bender, M. Elemental and isotopic composition of occluded O₂ and N₂ in polar ice. *J. Geophys. Res.* **94**, 5137–5150 (1989).
- Leuenberger, M. & Siegenthaler, U. Ice-age atmospheric concentration of nitrous oxide from an Antarctic ice core. *Nature* **360**, 449–451 (1988).
- Steig, E. J. *et al.* Synchronous climate changes in Antarctica and the North Atlantic. *Science* **282**, 92–95 (1998).

Acknowledgements. We thank G. Hargreaves and J. Fitzpatrick for help obtaining samples, and E. Steig and E. Brook for sharing their depth-age scales. This work was supported by the NSF and the Director's office at the Scripps Institution of Oceanography.

Correspondence and requests for materials should be addressed to H.J.S. (e-mail: hjsmith@aaas.org).